

Transient Modelling of a Controllable Low Pressure Accumulator in CO₂ Refrigeration Cycles

Marcos Bockholt¹ Wilhelm Tegethoff¹ Nicholas Lemke²
 Nils-Christian Strupp¹ Christoph Richter¹

¹Technical University Braunschweig, Institute of Thermodynamics
 Hans-Sommer-Str. 5, 38106 Braunschweig
 Email: m.bockholt@tu-bs.de

²TLK-Thermo GmbH
 Hans-Sommer-Str. 5, 38106 Braunschweig
 Email: n.lemke@tlk-thermo.de

Abstract

Low pressure accumulators are usually employed in mobile R744 HVAC units to assure reliable operating conditions and consequently to extend equipment life. Furthermore, the design parameters of accumulator, e.g. the oil bleed hole, influence the coefficient of performance (COP) of the refrigeration cycle. A poorly designed accumulator may lead to inefficient refrigeration cycles. Thus, accumulators with a variable oil bleed hole, also called controllable accumulators, may be employed to bring the system to optimal operating condition assuring good performance. The aim of this work is to implement a semi-empirical physically based transient Modelica controllable accumulator model, which is part of TIL (the TLK-I_fT-Library). Transient simulations are carried out to evaluate the impact of a controllable accumulator in an automotive refrigeration system.

Keywords: controllable accumulator; refrigeration cycle control; COP optimisation; fluid systems

1 Introduction

On January 2006 the EU agreed to vanish HFC-134a from air conditioning systems of new vehicle models from 1 January 2011. The natural refrigerant R744 is one of the promising candidates to replace R134a. Therefore, the actual vehicle refrigeration technology has to be optimized to reach the efficiencies using R134a. In fixed orifice tube R744 air-conditioning systems a low pressure accumulator is usually placed at

the compressor inlet in order to store excess refrigerant, allowing an optimum system performance under various ambient conditions and compensating refrigerant loss through leakage along the life cycle. The refrigerant quality at the accumulator inlet is also influenced by the oil bleed hole located in the “J” tube of the accumulator, see e.g. Fig. 3. The size of the oil bleed hole is an optimization parameter in accumulator design and should be variable to attend optimum performance for different operating conditions and avoid high compressor outlet temperatures. This variability of the oil bleed hole can be put into practice by building a controllable accumulator.

2 TIL

TIL is a new component model library for thermodynamic systems that was developed by the Institute for Thermodynamics (IfT) and the TLK-Thermo-GmbH and that allows for the steady-state and transient simulation of thermodynamic systems. The underlying design principles as well as a detailed description of selected component models is given by [4].

TIL provides component models for the simulation of refrigeration, air-conditioning, and heat-pump systems. Many component models use a formulation of the balance equations that is similar to the balance equations for the accumulator as presented in the following section. TIL uses the object-based fluid property library TILFluids for the computation of fluid properties. This fluid property library uses a generalized approach to include external fluid property com-

putation codes (e.g., REFPROP) in Modelica and a number of software tools.

3 Mathematical Modelling

Fig. 1 shows the control volume of the semi-empirical accumulator model V_{kv} . The following assumptions are made:

- The accumulator has adiabatic walls.
- The control volumes V_{kv}^1 are constant in time.
- Changes of kinetic and potential energy are not taken into account.
- The accumulator characteristics regarding the accumulated mass is modeled according to steady-state characteristic curves. The characteristic diagram determines the outlet enthalpy depending on the filling level.
- The accumulator outlet enthalpy may be changed by opening the oil bleed hole.
- Oil fraction in the liquid phase is ignored.

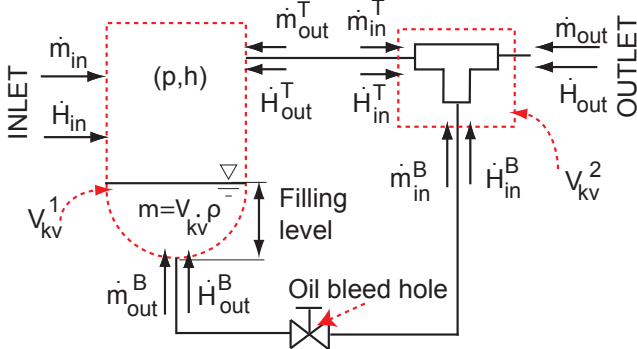


Figure 1: Controlled accumulator model.

3.1 Conservative Laws

3.1.1 Mass Balance

The transient mass balance equation for the control volume V_{kv}^1 is stated as follows:

$$\frac{dm}{dt} = \dot{m}_{in} + \dot{m}_{out}^T + \dot{m}_{out}^B \quad (1)$$

Eq. 1 can be stated as:

$$\begin{aligned} \frac{d}{dt}(\rho \cdot V_{kv}) &= \dot{m}_{in} + \dot{m}_{out}^T + \dot{m}_{out}^B \\ V_{kv} \cdot \frac{d\rho}{dt} &= \dot{m}_{in} + \dot{m}_{out}^T + \dot{m}_{out}^B \end{aligned}$$

Using the Bridgmann's table the derivative $\frac{d\rho}{dt}$ above can be split into:

$$\frac{d\rho}{dt} = \left. \frac{d\rho}{dh} \right|_p \cdot \frac{dh}{dt} + \left. \frac{d\rho}{dp} \right|_h \cdot \frac{dp}{dt}$$

The partial derivatives $\left. \frac{d\rho}{dh} \right|_p$ and $\left. \frac{d\rho}{dp} \right|_h$ are modeled in TILFluids for the one phase and two phase regions.

3.1.2 Energy Balance

The 1st. Law of Thermodynamics for an opened system in its transient form is applied to the control volume V_{kv}^1 resulting in the following differential equation:

$$\begin{aligned} \frac{dU}{dt} &= \dot{m}_{in} \cdot h_{in} + \dot{m}_{out}^T \cdot h_{out}^T + \dot{m}_{out}^B \cdot h_{out}^B \\ \frac{d}{dt}(H - p \cdot V_{kv}^1) &= \dot{H}_{in} + \dot{H}_{out}^T + \dot{H}_{out}^B \\ \frac{d}{dt}(m \cdot h) &= \dot{H}_{in} + \dot{H}_{out}^T + \dot{H}_{out}^B + V_{kv}^1 \cdot \frac{dp}{dt} \\ m \frac{dh}{dt} + h \frac{dm}{dt} &= \dot{H}_{in} + \dot{H}_{out}^T + \dot{H}_{out}^B + V_{kv}^1 \cdot \frac{dp}{dt} \quad (2) \end{aligned}$$

Using the mass balance Eq. 1, the Eq. 2 is rewritten into:

$$\begin{aligned} \frac{dh}{dt} &= \frac{1}{m} \cdot [\dot{m}_{in} \cdot (h_{in} - h) + \dot{m}_{out}^T \cdot (h_{out}^T - h) + \\ &+ \dot{m}_{out}^B \cdot (h_{out}^B - h) + V_{kv}^1 \cdot \frac{dp}{dt}] \quad (3) \end{aligned}$$

where h is the enthalpy of the in the accumulator accumulated refrigerant. The system of differential equations (see Eqs. 1 and 2) is reduced from $\left(\frac{dh}{dt}, \frac{dp}{dt}, \frac{dm}{dt}\right)$ to $\left(\frac{dh}{dt}, \frac{dp}{dt}\right)$ using the Bridgmann's table. This formulation has been shown to be very efficient for transient simulations (see [2, 7] for further details).

3.2 Accumulator

The semi-empirical accumulator model V_{kv}^1 in Fig. 1 is treated here in detail. Different from the existing TIL accumulator model, the model extended here is able to influence the outlet enthalpy and hereby to increase

or decrease the level of accumulated liquid refrigerant by opening the oil bleed hole. Basically, the accumulator's physical behavior is characterized by its filling level, a phase separation efficiency and an empirical characteristic diagram.

3.2.1 Filling level

The filling level is defined as the liquid fraction of the accumulated refrigerant:

$$\delta = 1 - \left(\frac{h - h_{liq}}{h_{vap} - h_{liq}} \right). \quad (4)$$

where h is the enthalpy of the accumulated refrigerant. The outlet enthalpy at the accumulator top h_{out} depends on this variable as shown in Sec. 3.2.3.

$$\delta = \begin{cases} \delta_{min} = 0 & \text{if the accumulator is empty.} \\ \delta_{drop} & \text{if fluid droplets occur} \\ & \text{at the accumulator outlet.} \\ \delta_{max} = 1 & \text{if the accumulator is flooded} \\ & \text{with saturated liquid.} \end{cases}$$

A detailed investigation is described in [5] for different accumulator geometries and operation conditions using a transparent accumulator.

3.2.2 Separation efficiency η_S

The accumulator separation efficiency η_S describes the ability of an accumulator in separating the refrigerant phases. It is defined as as follows:

$$\eta_S = x_{out} \quad (5)$$

where x_{out} is the accumulator outlet quality when the accumulator filling level is between the droplet filling level and the minimum filling level, $\delta_{min} \leq \delta \leq \delta_{drop}$. An ideal accumulator without an oil bleed hole would have a separation efficiency of 100%, i.e. only refrigerant vapor h_{vap} leaves the accumulator. The separation efficiency is strongly dependent on the oil bleed hole diameter and is estimated from steady-state measurement data, see [3, 5]. These data show that the separation efficiency may range from 75% up to 98%.

3.2.3 Characteristic diagram

The accumulator characteristic diagram is divided in four different operating conditions according to its filling level. These operating conditions are drawn as follows:

I) **Accumulator is nearly empty** ($\delta \leq \delta_{min}$): in this operation point no liquid droplet occurs from eventually accumulated refrigerant in the receiver and the refrigerant phases are separated. This means that if the refrigerant enters the accumulator with quality $x_{in} = 0.7$ it will leave it with quality $x_{out} = \eta_S = 1$. The liquid part begins to accumulate.

II) **Accumulator has a filling level with few liquid droplets at the outlet** ($\delta_{min} < \delta \leq \delta_{drop}$): if the droplet filling level δ_{drop} is not reached, a very small amount of liquid droplets from the accumulated refrigerant occurs at the outlet of the accumulator. The refrigerant phases are still separated and the accumulator outlet quality is the separation efficiency $x_{out} = \eta_S$. This is the most common operating condition and will be treated in the steady state simulation presented in a further section.

III) **Accumulator has a filling level with excess of liquid droplets at the outlet** ($\delta_{drop} < \delta \leq \delta_{max}$): for this operation point, the accumulated refrigerant in the accumulator has reached a level in that large amount of accumulated liquid starts to leave the accumulator. The refrigerant phases cannot be clearly separated. The outlet enthalpy starts to decrease and enters the two phase area ($x_{liq} < x_{out} < \eta_S < x_{vap}$).

IV) **Accumulator is full** ($\delta > \delta_{max}$): if the receiver reached this filling level, it is then flooded and there is no separation of the refrigerant phases. The liquid phase dominates in the receiver and the outlet enthalpy equals or is small than the saturated liquid enthalpy, i.e. $\eta_S = 0$. This is a vary rare operation condition and is out of the scope of this work.

3.3 Controllable accumulator

The controllable accumulator, is shown as an extension of the ideal accumulator of TIL. A prototype of a controllable accumulator is presented in Fig. 3. The "J"-tube with the oil bleed hole may be modeled by correlating the oil bleed hole in the "J"-tube with the separation efficiency stated in Eq. 5.

3.3.1 Oil bleed hole ϕ

To verify the effect of changing the oil bleed hole diameter in a standard accumulator a measurement

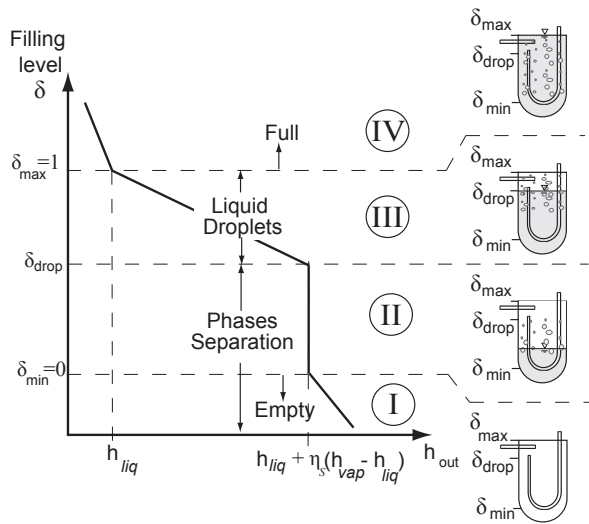


Figure 2: Accumulator characteristic diagram.

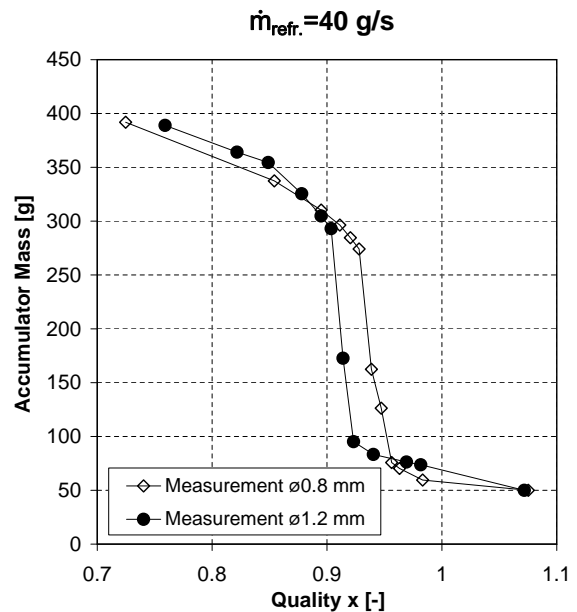


Figure 4: Accumulated mass dependence on the oil bleed hole, from [5].

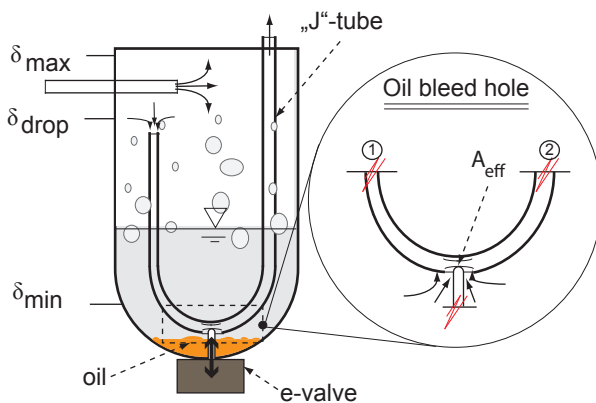


Figure 3: Accumulator prototype, from [1].

configuration developed by the Institut für Thermodynamik in Braunschweig, for the purpose of determining the liquid level in low-pressure accumulators with carbon dioxide as refrigerant is used. The measurements are performed varying the gas cooler outlet temperature yielding a variation of the accumulator outlet quality, see [5] for further details. In Fig. 4 it is observed that the accumulator outlet quality decreases by increasing the oil bleed hole diameter, i.e. reducing the separation efficiency. Thus, the separation efficiency will be used as a variation parameter to control the accumulator. A physical correlation between the efficiency and oil bleed hole should be further investigated in future works.

4 Steady-state simulation results

To investigate the impact of changing the accumulator efficiency in cycle behavior, a high ambient temperature and idle compressor speed condition for an automotive air-conditioning is applied. The refrigeration cycle characteristics and boundary conditions are summarized in the Tabs. 1 and 2. As a first approxi-

Total CO ₂ mass [kg]	Cycle internal volume [l]	Compressor displacement [cm ³]
0.5	1.5	28

Table 1: Cycle characteristics

Compressor speed [rpm]	\dot{m}_{air} evaporator [g/s]	\dot{m}_{air} gas cooler [g/s]	Ambient Temperature [°C]
780	140	600	40

Table 2: Boundary conditions for an automotive application

mation, the compressor volumetric and isentropic efficiencies as well as the heat transfer coefficients in the heat exchangers are kept constant for the cycle. The first step in this analysis is to find out the optimum operation pressure for the chosen boundary conditions and different accumulator efficiencies. Fig. 5 shows how the optimal high pressure varies with the accumu-

lator separation efficiency. The optimal high pressure is reached by setting the valve flow area 0.35 mm^2 . The result of the COP-optimized cycles for three different accumulator separation efficiency are summarized in Tab. 3. In Fig. 6 the COP-optimized cycle is shown in the pressure-enthalpy diagram for the accumulators with small, medium and large-sized oil bleed hole. The increase in the compressor suction density is observed in Fig. 6 at point 1, which is shifted to the two phase region when decreasing the accumulator separation efficiency. In order to keep the same suction density at the compressor inlet, an enhanced internal heat exchanger (IHX) with maximal thermodynamic efficiency is used. The result is shown in the pressure-enthalpy diagram in Fig. 7. Now, a change on the accumulator efficiency has neither effect on the system Coefficient of Performance (COP) nor changes its cooling capacity. The points 4 and 5 are shifted to the left at the same amount as the point 6. This fact evidences a dependence between the accumulator separation efficiency and the IHX heat transfer two-phase heat transfer effects.

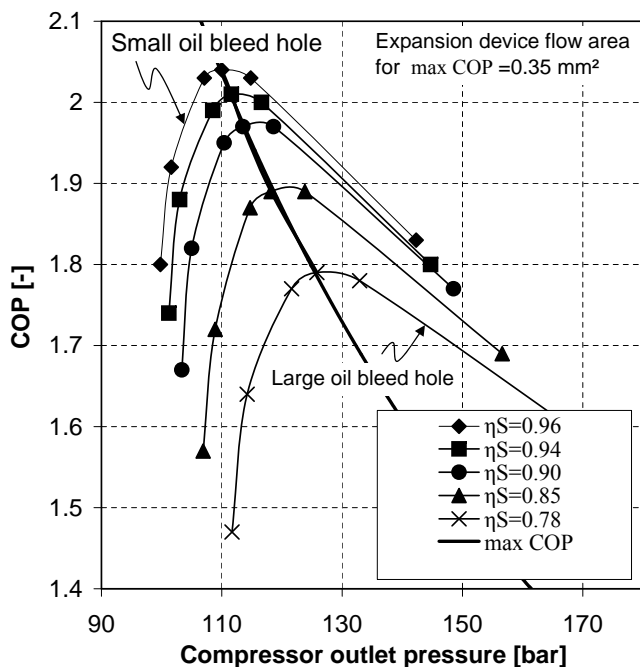


Figure 5: Coefficient of Performance (COP) sensitivity analysis for different accumulator separation efficiencies.

State variable	Unit	Separation efficiency η_s		
		0.78	0.85	0.96
$m_{CO_2 \text{ cycle}}$	[kg]	0.5	0.5	0.5
$m_{CO_2 \text{ accu}}$	[kg]	0.163	0.185	0.214
$x_{\text{accu out}}$	[-]	0.78	0.85	0.96
$T_{\text{comp out}}$	[°C]	91.4	94.5	100.9
$\dot{m}_{CO_2 \text{ cycle}}$	[g/s]	37.7	35.1	31.6
$p_{\text{comp out}}$	[bar]	125.8	118.2	110.0
$\Delta \dot{H}_{\text{air}}$	[kW]	3.38	3.34	3.26
IHX $\Delta \dot{H}_{\text{ref}}$	[kW]	1.4	1.3	1.1
COP	[-]	1.79	1.89	2.04

Table 3: Impact of the separation efficiency in steady-state cycle simulation.

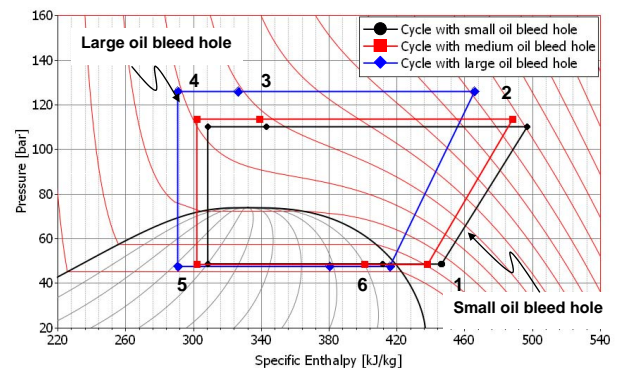


Figure 6: Pressure-enthalpy (p-h) diagram for COP-optimized cycles with large, medium and small oil bleed hole.

5 Transient simulation of a CO₂ refrigeration cycle with a controllable accumulator

In this application, a controllable accumulator is used to avoid that the temperature at the compressor outlet $T_{\text{comp out}}$ exceeds the oil decomposition temperature, e.g. $160 \text{ }^\circ\text{C}$. The cycle used previously for the steady state simulation, see Fig. 8, is now used in a transient simulation, where the compressor speed is set to $n = 2100 \text{ rpm}$ and the gas cooler and evaporator air inlet temperature $T_{\text{evap in}}$ are assumed to be $40 \text{ }^\circ\text{C}$. Fig. 9 shows the results of the transient simulation for some of the state variables. At time $t = 50 \text{ s}$ the

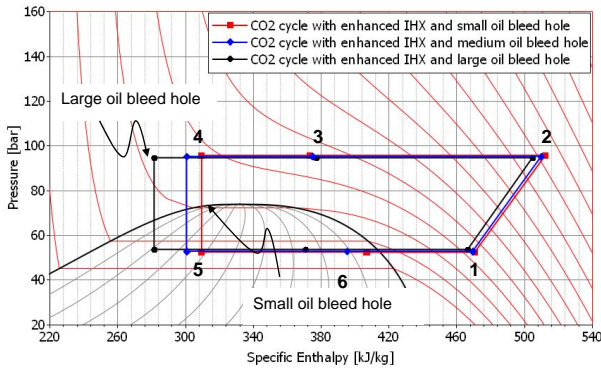


Figure 7: Pressure-enthalpy (p-h) diagram for COP-optimized cycles with large, medium and small oil bleed hole and enhanced IHX, with heat exchange area ($A_{IHX} \approx \infty$).

separation efficiency of the accumulator is decreased from $\eta_s=96\%$ to $\eta_s=78\%$, compare $\eta_s = x_{out}$ in Fig. 9. Some refrigerant mass in the accumulator m_{accu} is moved to the cycle high-side pressure. The suction density at the compressor inlet increases yielding a higher compressor shaft power P_{comp} . An increase in P_{comp} means a decrease in the system coefficient of performance $COP = \Delta \dot{H}_{air} / P_{comp}$ as observed in Fig. 9. The compressor outlet temperature is decreased to a value smaller than the maximum oil working temperature. The increase in the cycle refrigerant mass flow rate due to higher compressor suction densities causes an insignificant increase in the cooling capacity for this modeling assumptions. The evaporator air outlet temperature $T_{air\ evap\ out}$ increases slightly.

6 Conclusion

The transient model of a controllable accumulator is presented to investigate the effects of varying the separation efficiency in an automotive CO₂ refrigeration. The model consists of simple models from the new component model library for thermodynamic systems that was developed by the Institute for Thermodynamics (IfT) and the TLK-Thermo-GmbH. The mathematical formulation used in the modeling allows an accelerated analysis of the parametric variation.

The results from the steady state simulation show a strong dependency between the accumulator separation efficiency and the internal heat exchanger (IHX) efficiency if the system Coefficient of Performance (COP) is considered. In a first simulation run with constant heat transfer coefficients in the heat ex-

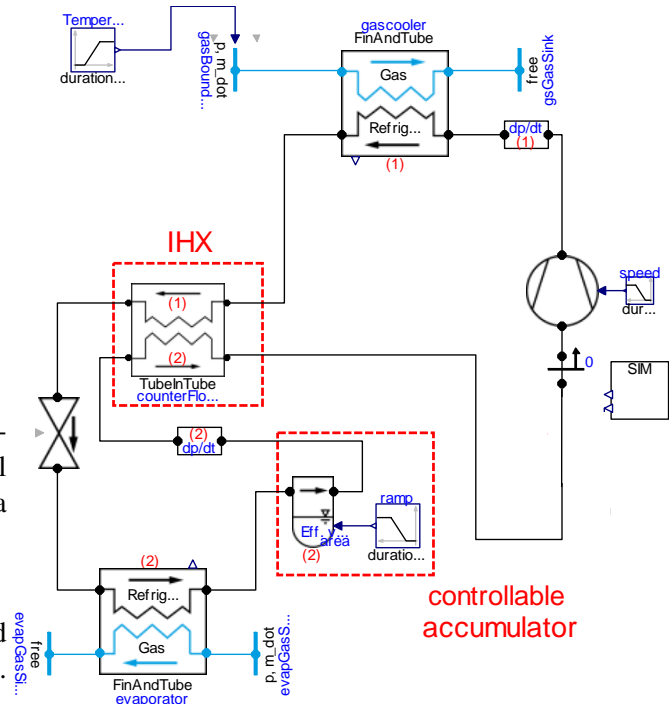


Figure 8: CO₂ refrigeration cycle with controllable accumulator using component models from TIL.

changes it was observed an increase in the system COP when closing the oil bleed hole. Otherwise, if the oil bleed hole is opened the compressor outlet temperature decreases avoiding the oil temperature to reach critical limits. A second simulation run showed that using a nearly optimal IHX the oil bleed hole variation has no effect in the cycle COP and cooling capacity.

A transient simulation is carried out for a an automotive air-conditioning boundary condition. As a first application, it is shown that the compressor outlet temperature may be kept under the oil critical limit without loss of cooling capacity.

Future work will concentrate on finding an optimal relationship between IHX efficiency and accumulator separation efficiency as well an optimal control strategy for a CO₂ refrigeration cycle using this innovative component. Two-phase heat transfer effects in the IHX and in the other cycle heat exchangers should be taken into account in order to predict the cycle behavior more accurately when varying the accumulator oil bleed hole. The isentropic and volumetric compressor efficiencies should also be mapped more accurately so that the cycle mass flow rate and compressor outlet temperature can be precisely estimated.

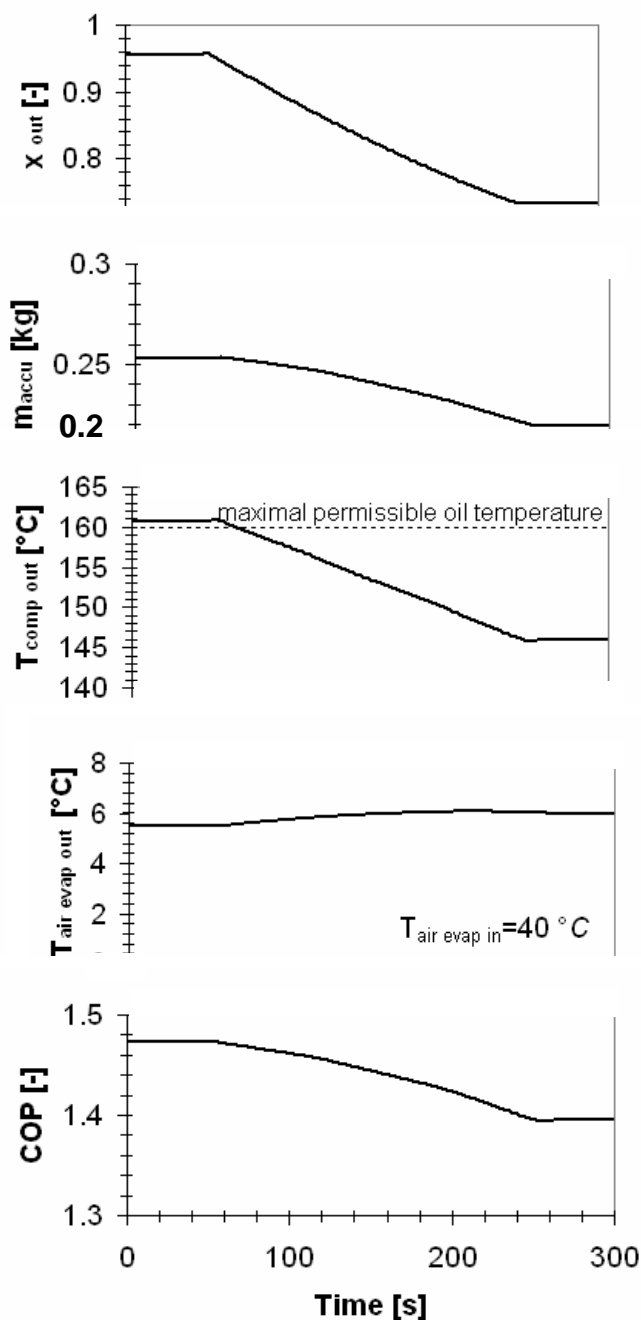


Figure 9: Simulation results of the transient controllable accumulator model in a CO₂ refrigeration cycle

References

- [1] Hirota, H.: *Refrigeration cycle*, European Patent Application EP 1607698 A2, TGK Company Ltd., Tokyo, 2005
- [2] Lemke N.: *Untersuchung zweistufiger Flüssigkeitskühler mit dem Kältemittel CO₂*, PhD thesis, TU-Braunschweig, Institute of Thermodynamics, 2005.
- [3] Raiser H., Heckenberger T., Tegethoff T., Försterling S.: *Transient Behavior of R744 Vehicle Refrigeration Cycles and the Influence of the Suction Side Accumulator Design*, SAE International, Nr. 2006-01-0162, 2006.
- [4] Richter C.: *Proposal of New Object-Oriented Equation-Based Model Libraries for Thermodynamic Systems*, TU Braunschweig, PhD-thesis, 2008
- [5] Strupp C., Lemke N., Tegethoff T., Köhler J.: *Investigation of Low Pressure Accumulators in CO₂ Refrigeration Cycles*, International Congress of Refrigeration, Beijing, China, ICR07-E1-1480, 2007.
- [6] Tegethoff W.: *Eine objektorientierte Simulationsplattform für Kälte-, Klima- und Wärmepumpensysteme*, PhD thesis, TU-Braunschweig, Institute of Thermodynamics, 1999.
- [7] Tegethoff W., Lemke N., Correia C., Cavalcante P., Köhler J.: *Component modelling and specification using a new approach for transient simulation*, VDA Alternate Refrigerant Refrigerant Winter Meeting- Automotive Air-Conditioning and Heat Pump Systems, 2004